

► Inductance et al.—A Closer Look at AC, Part 2

By Steve Mowry

THE AC PROBLEM

I will pick up this discussion of inductance factors within the motor assembly with perhaps the most dreaded of all equations, Maxwell's AC electromagnetic vector equation in integral form!

$$\oint E \cdot dl = -\iint Tm \cdot dS - \frac{d}{dt} \iint B \cdot dS(V) \quad (11)$$

All this means is that the electric field E (V/m) is related to the magnetic charge density, Tm (V/m²) and the time varying AC flux density, (Wb/m²s) or (T/s). Fortunately, for this case you can simplify the equation, but as in the DC problem these are nonlinear electromagnetic quantities that depend on voice coil position, x , and current, i .

$$-E(x) = \frac{J}{\sigma}(x) + \frac{d}{dt} \frac{\phi}{2\pi r}(x,i) \quad (12)$$

where J (A/m²) is the "AC eddy current density"; r is the radius, (m); σ is the electrical conductivity (1/ Ω m), and $\frac{d\phi}{dt}$ (Wb/s) is the time varying magnetic flux.

What this means is that where there is an AC electric field, there is current and a time varying magnetic field. Remember that all those loudspeaker magnets are DC permanent magnets. The DC magnetic field does not change with time.

In the copper or aluminum shorting ring(s) where $\mu = \mu_0$ (Fig. 2 in Part 1), the permeability of air (H/m), the induction is small and is assumed zero. While in the magnet, the conductivity, σ , is quite small and $\mu = \mu_0$, thus the AC induction is assumed zero and the resistivity, $1/\sigma$, is large. Thus the magnet is treated as air with regard to the AC model segment. Remember that the AC magnetic fields are the results of the AC current i in the voice coil.

Then the AC voltage in the voice coil produces an AC electric field and thus an AC eddy current density, J , and time varying flux result within the motor assembly. Figures

9-14 in Part 1 illustrate these quantities and show that they change with voice coil position and the skin depth changes with frequency. This is illustrated in the left-hand segment of the model in Fig. 1.

The AC problem is inherently separate from the DC problem in that the DC flux and the DC flux density do not change with time:

$$\frac{dB}{dt} = 0 \text{ and } \frac{d\phi}{dt} = 0 \quad (13)$$

The AC magnetic field does change with time:

$$\frac{dB}{dt} \neq 0 \text{ and } \frac{d\phi}{dt} \neq 0 \quad (14)$$

$\frac{d}{dt}$ is the notation for the rate of change of a quantity with respect to time, (1/s).

The *VECTOR FIELDS* PC OPERA 2d finite element analysis software restarts the AC steady-state harmonic analysis from the DC permeability. Subsequently, the solution to the DC and AC problems can be displayed separately. Look at the steady-state solutions to the AC problem to further explain the dynamic permeability and other AC phenomena.

Figures 17-22 contain plots of the eddy current density, $J(x)$ at $x = X_{max}$, 0 and $-X_{max}$ at 100 and 1000Hz. It is clear that the eddy current density changes with voice coil position, x .

Figures 23-28 contain contours of the AC flux lines, $\phi(x)$, that illustrate that the AC magnetic field changes with voice coil position and frequency as the skin depth, δ , changes. The peak $|B|$ is also plotted on the color scale but the flux lines hide the skinned AC flux density.

The inductance, L_e , is simply the total AC flux linkage, $N\phi$ (Wb) with respect to the voice coil divided by the AC current, i (A) (equation 15), where N is the number of turns

of voice coil wire.

$$L_e = \frac{N\phi}{i} \quad (15)$$

Inductance and the AC force factor are related by the change in flux linkage with voice coil position divided by the voice coil wind height (equation 16). This is displayed in **Fig. 42**.

$$\frac{dL_e(x)i}{dx} = \frac{Nd\phi(x)}{dx} = \frac{N[\phi(x+dx/2) - \phi(x-dx/2)]}{dx} = Bl(x) \quad (16)$$

The command used to simulate inductance as illustrated in **Fig. 41** is shown in equation 17.

$$L_e(x) = N \int \frac{\phi(x)}{i} = \frac{N[\phi(x+dx/2) + \phi(x-dx/2)]}{2i} \quad (17)$$

The integration is just a moving average of the AC flux but with respect to the voice coil height, dx . However, equations 15 and 16 should be displaced and applied piecewise, three

pieces minimum, to the finite element models for the most accurate simulation.

Just as the DC flux density linking to current in the voice coil results in a force, the AC flux density also links to the current in the voice coil (**Fig. 42**), which results in an AC reluctance force. For a sinusoidal signal, the reluctance force, shown in equation 18, also depends on the skin depth.

$$F_m(\delta, x, i) = \frac{Bl(\delta, x, i)i}{2} (N) \quad (18)$$

With the shorting ring, the eddy current density within the steel is decreased and copper does not skin at audio frequencies. As frequency increases the shorting ring is more effective. The ferromagnetic material is skinning and the shorting ring is essentially shorting the inductance (Fig. 1).

EDDY CURRENT LOSS

The resistance that the voice coil sees as a result of the AC eddy current within the silver, copper, or aluminum-shortening ring is shown in relationship 19.

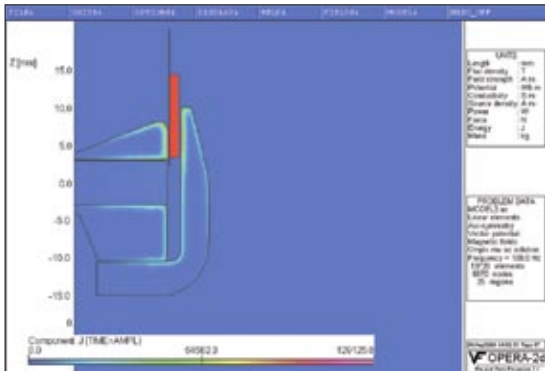


FIGURE 17: Contour plot of eddy current density $|J|$ at 100Hz, $x = X_{max}$, $i = 24A$.

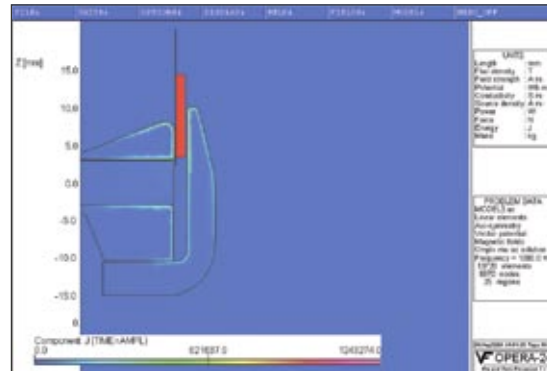


FIGURE 20: Contour plot of eddy current density $|J|$ at 1.0kHz, $x = X_{max}$, $i = 24A$.

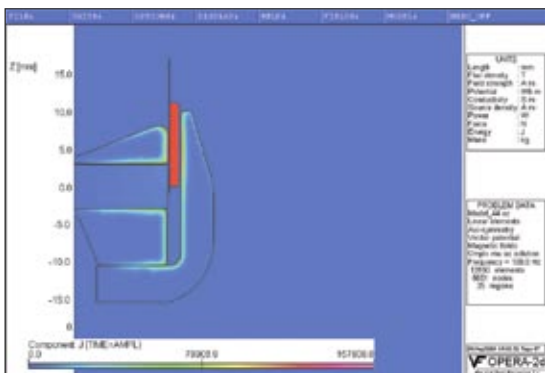


FIGURE 18: Contour plot of eddy current density $|J|$ at 100Hz, $x = 0$, $i = 24A$.

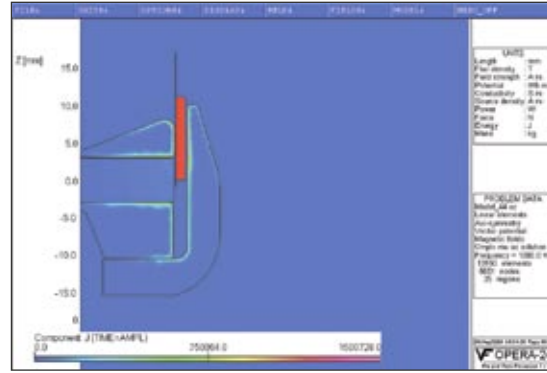


FIGURE 21: Contour plot of eddy current density $|J|$ at 1.0kHz, $x = 0$, $i = 24A$.

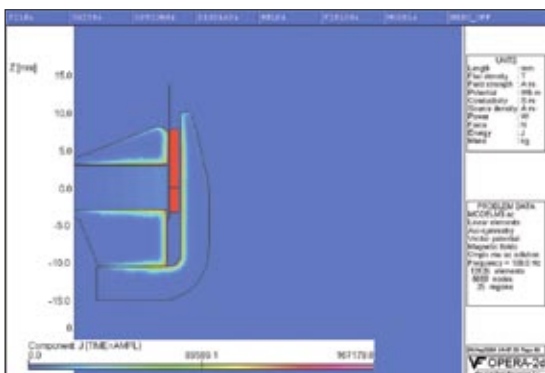


FIGURE 19: Contour plot of eddy current density $|J|$ at 100Hz, $x = X_{max}$, $i = 24A$.

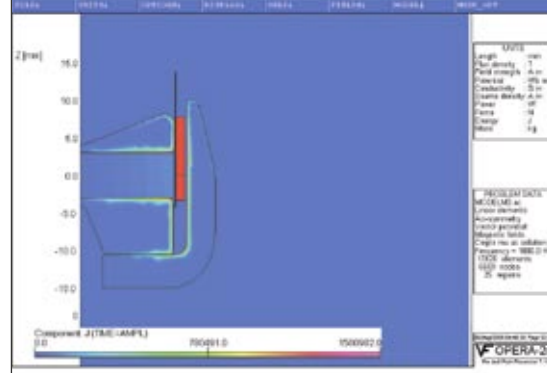


FIGURE 22: Contour plot of eddy current density $|J|$ at 1.0kHz, $x = -X_{max}$, $i = 24A$.

$$R_{SR} \alpha \frac{2\pi r}{\sigma_{SR} \cdot S_{SR}} (\Omega) \quad (19)$$

Where typically the radius of the shorting ring/shorted turn is approximately equal to the radius of the voice coil; the high conductivity of the shorting ring does, in effect, short the eddy current especially as frequency is increased; and the steel skin depth becomes small. To further improve the linearization due to the shorting ring at low frequencies, increase the cross-section, S_{SR} . A real challenge with shorting ring design can be strategic placement. Real estate within the magnetic gap is critical, and typically the thickness is limited to 0.30mm (0.012"). However, there are alternatives to placing the ring in the gap and you can select many other combinations of geometry and materials.

Figures 29-31 and **Figs. 35-37** illustrate the eddy current density, J_{SR} , within the shorting at 100 and 1000Hz, respectively. You can observe that the eddy current density changes somewhat with voice coil position, x . The current density in the shorting ring increases at 1000Hz; however,

the current density in the steel decreases!

The permeability of the shorting ring is μ_0 , the permeability of air. I ignored any frequency or current dependent skin effect. The resistance the voice coil sees due to eddy current losses within the shorting ring goes as the ratio of the length of the ring, the circumference to the cross-section times the conductivity of the shorting ring. Oxygen-free copper and aluminum are the most common materials for these rings; however, you can also use silver. The conductivity of these materials is high, while silver is the highest of all.

The resistance the voice coil sees as a result of the AC eddy current within the ferromagnetic material depends on the skin depth and is shown in relationship 20.

$$R_{FM}(\delta) \alpha \frac{2\pi r}{\sigma_{FM} \cdot S_{FM}} \sim \frac{2\pi r}{\sigma_{FM} \cdot (x_0 + \delta)} (\Omega) \quad (20)$$

As the skin depth δ is reduced, the resistance will increase. $z_0 + \delta$ and $r_0 + \delta$ are the vertical and horizontal skin sections, respectively, in the contours of AC eddy current density illustrated in **Figs. 17-22**. The cross-section, S_{FM} , is

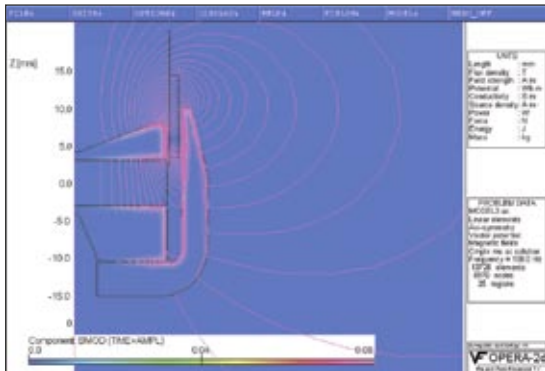


FIGURE 23: Contour plot of AC flux lines, ϕ at 100Hz, $x = X_{max}$, $i = 24A$.

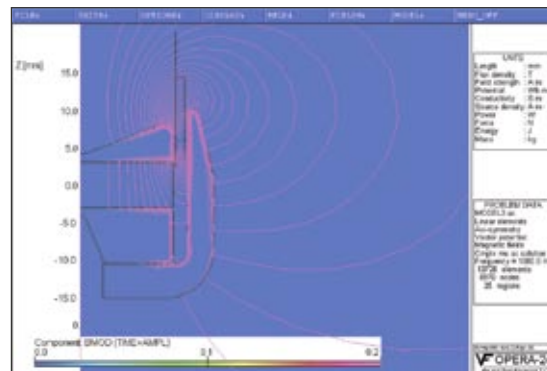


FIGURE 26: Contour plot of AC flux lines, ϕ at 1.0kHz, $x = X_{max}$, $i = 24A$.

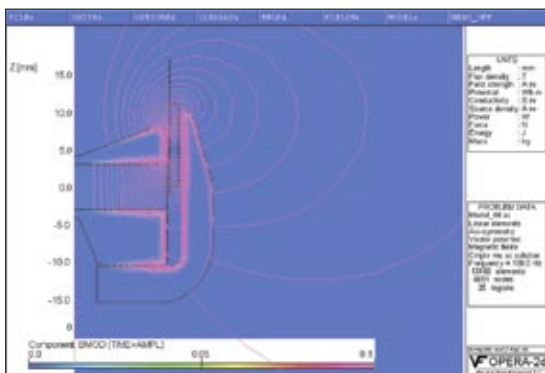


FIGURE 24: Contour plot of AC flux lines, ϕ at 100Hz, $x = 0$, $i = 24A$.

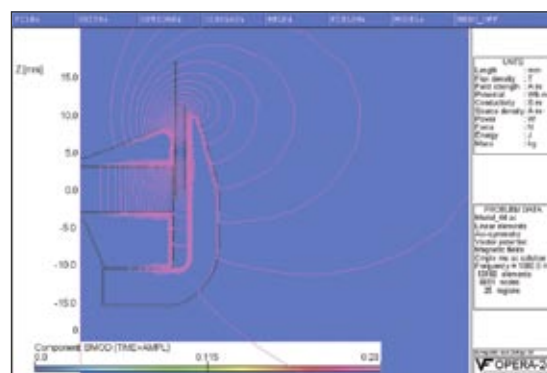


FIGURE 27: Contour plot of AC flux lines, ϕ at 1.0kHz, $x = 0$, $i = 24A$.

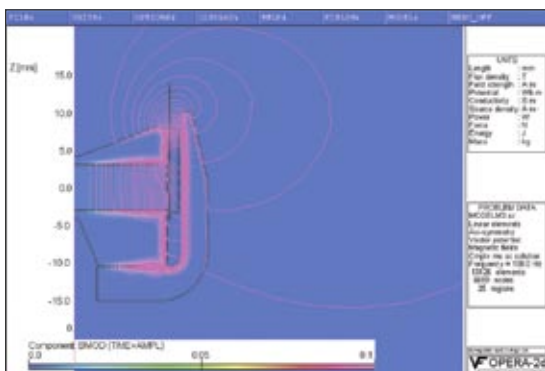


FIGURE 25: Contour plot of AC flux lines, ϕ at 100Hz, $x = -X_{max}$, $i = 24A$.

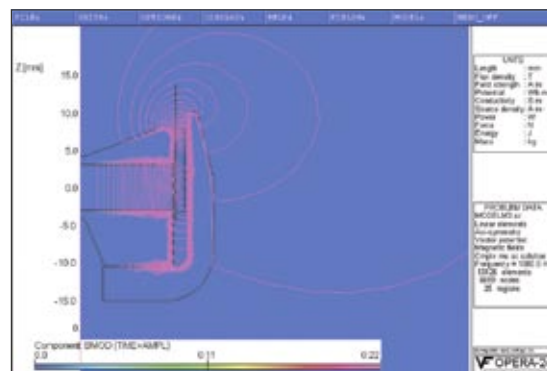


FIGURE 28: Contour plot of AC flux lines, ϕ at 1.0kHz, $x = -X_{max}$, $i = 24A$.

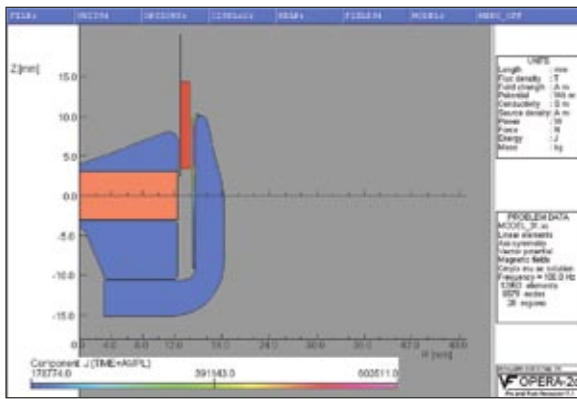


FIGURE 29: Contour plot of $|J_{SR}|$ within shorting ring only at 100Hz, $x = X_{max}$, $i = 24A$.

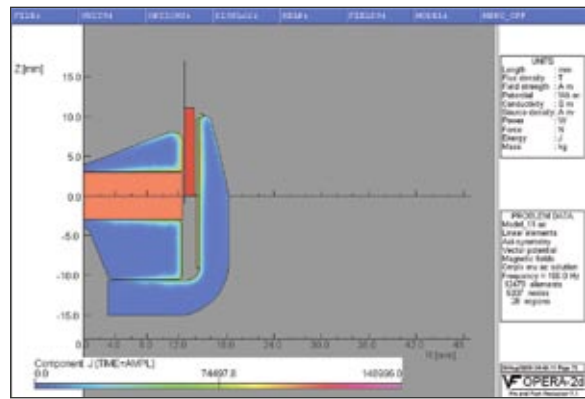


FIGURE 33: Contour plot of $|J_{FM}|$ within the steel only at 100Hz, $x = 0$, $i = 24A$.

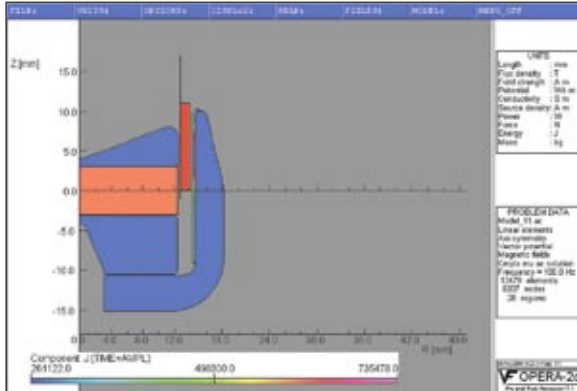


FIGURE 30: Contour plot of $|J_{SR}|$ within shorting ring only at 100Hz, $x = 0$, $i = 24A$.

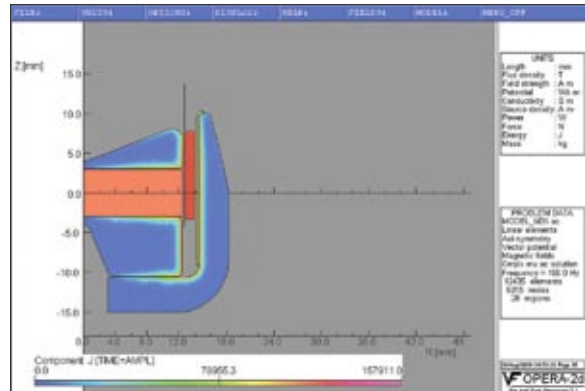


FIGURE 34: Contour plot of $|J_{FM}|$ within the steel only at 100Hz, $x = -X_{max}$, $i = 24A$.

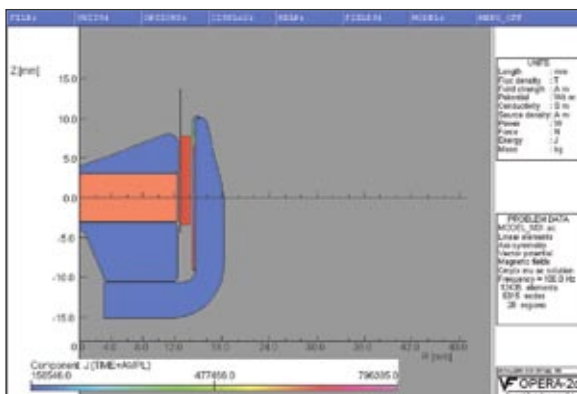


FIGURE 31: Contour plot of $|J_{SR}|$ within shorting ring only at 100Hz, $x = -X_{max}$, $i = 24A$.

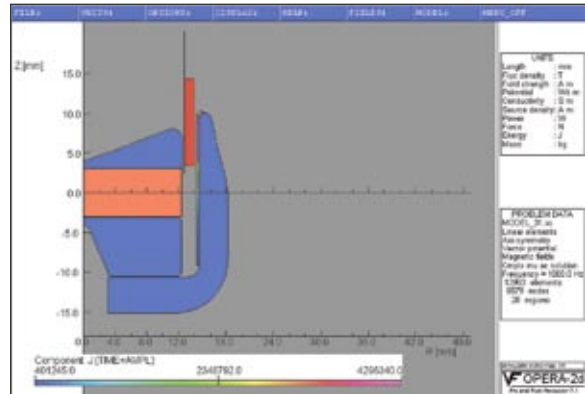


FIGURE 35: Contour plot of $|J_{SR}|$ within shorting ring only at 1.0kHz, $x = X_{max}$, $i = 24A$.

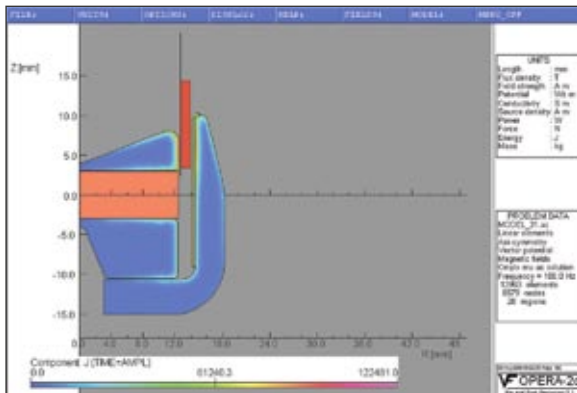


FIGURE 32: Contour plot of $|J_{FM}|$ within the steel only at 100Hz, $x = X_{max}$, $i = 24A$.

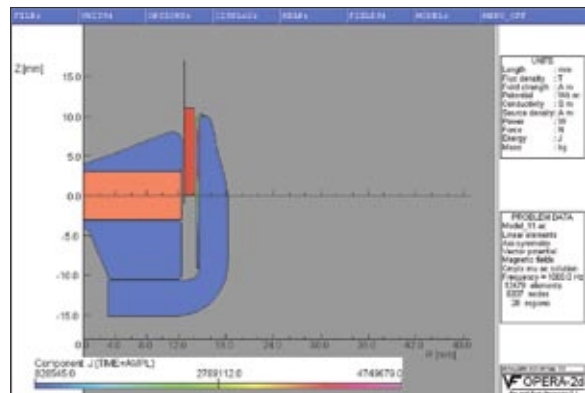


FIGURE 36: Contour plot of $|J_{SR}|$ within shorting ring only at 1.0kHz, $x = 0$, $i = 24A$.

effectively reduced. The eddy current losses then go inversely as the conductivity, σ_{FM} , and the skinned cross-section. The function of the shorting ring is to reduce the effective resistance and inductance, thus the eddy current within the steel due to the current division. This is clearly indicated by the model illustrated in Fig. 1, and you can see it in **Figs. 32-34** and **Figs. 38-40**. These quantities are material dominated and are best controlled with a shorting ring(s). The objective is to short the R_{FM} and the L_e with the high conductivity (low resistance copper or aluminum). This typically reduces loss and inductance.

CONCLUSION

I have presented a detailed discussion of the AC electromagnetic phenomenon and developed a model that relates to materials, geometry, and the voice coil within the motor assembly. When you use this model with finite element analysis and command files, a powerful simulation and design tool is realized. The modeling goes quickly and typically a complete motor design can be completed in one to two weeks. Motor nonlinearities are identified in such a way as to assist the transducer designer in quickly obtaining meaningful motor assembly information.

Within the DC problem the major nonlinear mechanism is the voice coil displacement $x(t)$ resulting from the AC current, $i(t)$. Within the AC problem the voice coil displacement, $x(t)$, is still a nonlinear mechanism; however, the magnetic field density is also changing with time, $B(x,t)$. Then it follows that the AC eddy current density is also changing with voice coil position and time, $J(x,t)$, because the eddy current is the major source of the AC flux, $\phi(x,t)$. If that wasn't enough, I have shown that these AC quantities also change with current, i , $\phi(x,i,t)$ and $B(x,i,t)$ due to changes in the dynamic permeability, $\mu(i,t)$. Finally, there is the AC skin effect in steel that adds losses and changes in eddy current density, $J(\delta,x,t)$ and changes in flux, $\phi(\delta,x,i,t)$, where $\delta \propto \frac{1}{\sqrt{f}}$ in the limit.

These are the nonlinear mechanisms within the motor assembly. The AC mechanisms are essentially all related to inductance and inductance modulation. If this is all starting to seem chaotic, it's not surprising. Nonlinearity and distortion are chaos. **VC**

Download my BH Curve text files at
www.s-m-audio.com/SM_Audio_BH_Curves.zip

Download my material property table including conductivity, σ , for common motor assembly materials at
www.s-m-audio.com/ENGINEERING_MATERIAL_PROPERTIES.zip

Download my Voice Coil Worksheet at
www.s-m-audio.com/SM_AUDIO_VOICE_COIL_WORKSHEET.zip

A special thanks to the technical staff at Advanced Sound Technology Sdn. Bhd. (MSC) for their support. Happy inductance modeling.

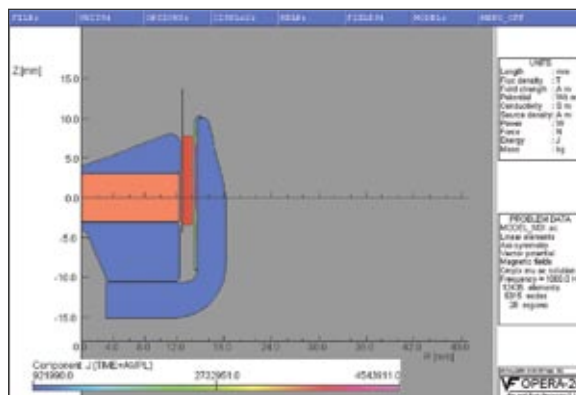


FIGURE 37: Contour plot of $|J_{SR}|$ within shorting ring only at 1.0kHz, $x = -X_{max}$, $i = 24A$.

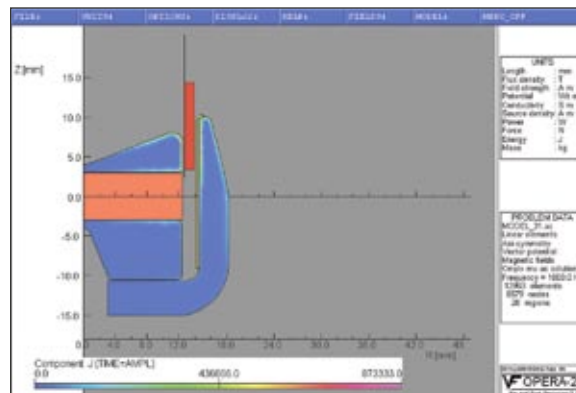


FIGURE 38: Contour plot of $|J_{FM}|$ within the steel at 1.0kHz, $x = X_{max}$, $i = 24A$.

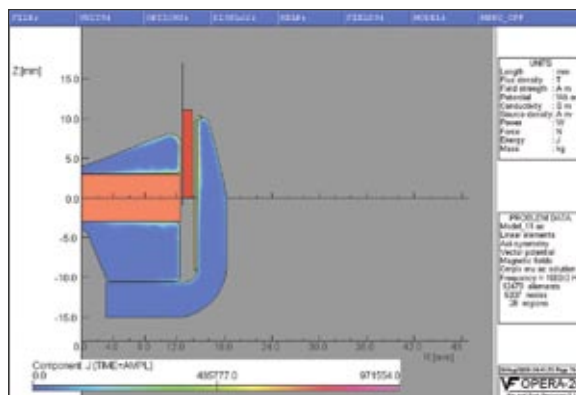


FIGURE 39: Contour plot of $|J_{FM}|$ within the steel only at 1.0kHz, $x = 0$, $i = 24A$.

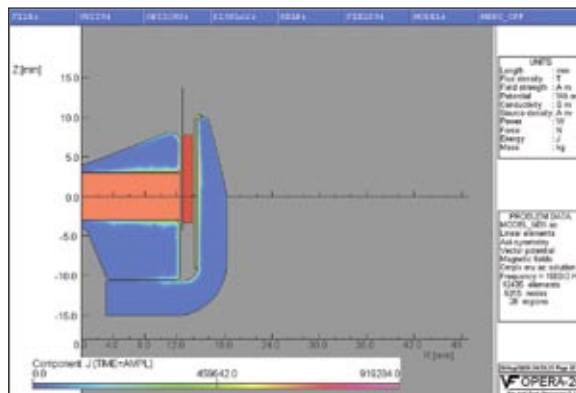


FIGURE 40: Contour plot of $|J_{FM}|$ within the steel only at 1.0kHz, $x = -X_{max}$, $i = 24A$.

Steve Mowry, president of SM Audio Engineering, has a BS, Business Administration, from Bryant College, and a BS and MS, Electrical Engineering, from URI with highest distinction. Steve has worked in R&D at BOSE, TC Sounds, EASTTECH, and PAudio. Steve is currently an independent consultant/lecturer in project management/transducer and system design. His website is www.s-m-audio.com.

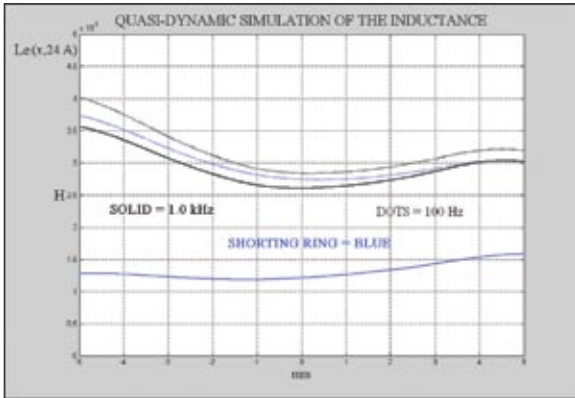


FIGURE 41: Quasi-dynamic simulation of inductance, $|L_e(x, 24A)|$ at 24A at 100Hz and 1.0kHz with and without shorting ring.

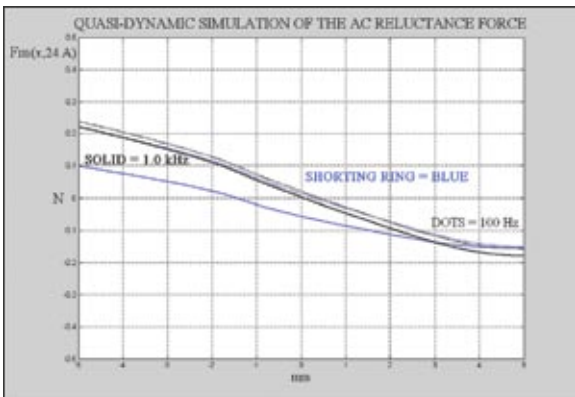


FIGURE 42: Quasi-dynamic simulation of the AC reluctant force, $F_m(x, 24A)$ at 24A at 100Hz and 1.0kHz with and without shorting ring.